REPORT DOCUMENTATION PAGE

Form Approved OMB NO. 0704-0188

The public reporting burden for this collection of information is estimated to average 1 hour per response, including the time for reviewing instructions, searching existing data sources, gathering and maintaining the data needed, and completing and reviewing the collection of information. Send comments regarding this burden estimate or any other aspect of this collection of information, including suggesstions for reducing this burden, to Washington Headquarters Services, Directorate for Information Operations and Reports, 1215 Jefferson Davis Highway, Suite 1204, Arlington VA, 22202-4302. Respondents should be aware that notwithstanding any other provision of law, no person shall be subject to any oenalty for failing to comply with a collection of information if it does not display a currently valid OMB control number.
PLEASE DO NOT RETURN YOUR FORM TO THE ABOVE ADDRESS.

1. REPORT DATE (DD-MM-YYYY)	2. REPORT TYPE	3. DATES COVERED (From - To)
	Technical Report	-

4. TITLE AND SUBTITLE
Development of Energy-Efficient Single-Electron Transistors with Oxide Nanoelectronics

5a. CONTRACT NUMBER
W911NF-09-1-0258

5b. GRANT NUMBER

5c. PROGRAM ELEMENT NUMBER
8G10AZ

6. AUTHORS
Jeremy Levy

5d. PROJECT NUMBER

5e. TASK NUMBER

5f. WORK UNIT NUMBER

7. PERFORMING ORGANIZATION NAMES AND ADDRESSES
University of Pittsburgh
123 University Place
University Club
Pittsburgh, PA 15213 -2303

8. PERFORMING ORGANIZATION REPORT NUMBER

9. SPONSORING/MONITORING AGENCY NAME(S) AND ADDRESS(ES)
U.S. Army Research Office
P.O. Box 12211
Research Triangle Park, NC 27709-2211

10. SPONSOR/MONITOR'S ACRONYM(S)
ARO

11. SPONSOR/MONITOR'S REPORT NUMBER(S)
56685-PH-DRP.1

12. DISTRIBUTION AVAILIBILITY STATEMENT
Approved for Public Release; Distribution Unlimited

13. SUPPLEMENTARY NOTES
The views, opinions and/or findings contained in this report are those of the author(s) and should not contrued as an official Department of the Army position, policy or decision, unless so designated by other documentation.

14. ABSTRACT
We report progress in creating nanoscale transistors at the LaAlO3/SrTiO3 interface using a rewritable conductive AFM technique. We have created LaAlO3/SrTiO3-based nano-transistors (SketchFETs) that operate at GHz frequencies. We have also demonstrated nanoscale phototransistors that are spectrally sensitive to visible and near-infrared light. We have also investigated the creation of "designer potential barriers" that allow the creation of nanoscale diodes. Finally, we have tested a physical model of the AFM writing mechanism, which shows that

15. SUBJECT TERMS
oxide nanoelectronics sketchfet transistor

16. SECURITY CLASSIFICATION OF:			17. LIMITATION OF ABSTRACT	15. NUMBER OF PAGES	19a. NAME OF RESPONSIBLE PERSON
a. REPORT	b. ABSTRACT	c. THIS PAGE			Jeremy Levy
UU	UU	UU	UU		19b. TELEPHONE NUMBER 412-624-2736

Report Title

Development of Energy-Efficient Single-Electron Transistors with Oxide Nanoelectronics

ABSTRACT

We report progress in creating nanoscale transistors at the LaAlO3/SrTiO3 interface using a rewritable conductive AFM technique. We have created LaAlO3/SrTiO3-based nano-transistors (SketchFETs) that operate at GHz frequencies. We have also demonstrated nanoscale phototransistors that are spectrally sensitive to visible and near-infrared light. We have also investigated the creation of "designer potential barriers" that allow the creation of nanoscale diodes. Finally, we have tested a physical model of the AFM writing mechanism, which shows that water vapor is an essential component to make these structures - an important step in developing devices in this material. For the remaining period we will further investigate the high frequency properties and SketchFETs, with a goal of quantifying power dissipation per drive cycle in these devices. We will also continue to develop single-electron transistor devices.

REPORT DOCUMENTATION PAGE (SF298)
(Continuation Sheet)

Development of Energy-Efficient Single-Electron Transistors with Oxide Nanoelectronics

Interim Progress Report

(1) Submissions or publications under ARO sponsorship during this reporting period. List the title of each and give the total number for each of the following categories:

1. Papers published in peer-reviewed journals

1. D. F. Bogorin, C. W. Bark, H. W. Jang, C. Cen, C. M. Folkman, C.-B. Eom, and J. Levy, *Nanoscale rectification at the $LaAlO_3/SrTiO_3$ interface*, Appl. Phys. Lett. **97** 013102 (2010)

2. Papers published in non-peer-reviewed journals

(none)

3. Presentations

i. Presentations at meetings, but not published in Conference Proceedings

1. J. Levy, *Oxide Nanoelectronics*, SUNY Buffalo, Buffalo, NY, September 17, 2009
2. J. Levy, *Oxide Nanoelectronics*, Vancouver, BC, Canada, September 24, 2009
3. J. Levy, *Oxide Nanoelectronics*, Tarragona, Spain, October 7, 2009
4. J. Levy, *Oxide Nanoelectronics*, IBM TJ Watson Center, New York City, NY , October 20, 2009
5. J. Levy, *Etch-a-Sketch Nanoelectronics*, AAPT Texas Section, San Marcos, TX, October 24, 2009
6. J. Levy, *Oxide Nanoelectronics*, University of Pennsylvania, Philadelphia, PA, November 4, 2009
7. J. Levy, *Oxide Nanoelectronics*, Florida State University, Tallahassee, FL, November 5, 2009
8. J. Levy, *Oxide Nanoelectronics*, University of North Carolina, Chapel Hill, NC, November 8, 2009
9. J. Levy, *Oxide Nanoelectronics on Demand*, Duke University, Raleigh, NC, November 10, 2009
10. J. Levy, *Oxide Nanoelectronics*, University of Wisconsin, Madison, WI, November 12, 2009
11. J. Levy, *Oxide Nanoelectronics*, University of South Florida, Tampa, FL, November 13, 2009
12. J. Levy, *Oxide Nanoelectronics*, University of Minnesota, Minneapolis, MN, November 18, 2009
13. J. Levy, *Possible observation of integer and fractional quantum hall states in an interfacial oxide nanostructure*, University of Minnesota, Minneapolis, MN, November 19, 2009
14. J. Levy, *Oxide Nanoelectronics*, Argonne National Laboratory, Chicago, IL, November 25, 2009
15. J. Levy, *Oxide Nanoelectronics*, University of California, Davis, Davis, CA, December 6, 2009
16. J. Levy, *Oxide Nanoelectronics: A New Platform for Quantum Information Technology*, Kavli Institute for Theoretical Physics, University of California, Santa Barbara, Santa Barbara, CA, December 10, 2009

17. J. Levy, *Etch-a-Sketch Nanoelectronics*, Aspen Center for Physics, Aspen, CO, February 3, 2010
18. J. Levy, C. Cen, D. F. Bogorin, *Quantum Transport in Oxide Nanostructures*, APS March Meeting 2010, Portland, OR, March 18, 2010
19. C. Cen, D. F. Bogorin, J. Levy, *Weak Antilocalization and Spin-Orbit Coupling in $LaAlO_3/SrTiO_3$ Nanostructures*, APS March Meeting 2010, Portland, OR, March 16, 2010
20. V. Srinivasa, J. Levy, C. Cen, *Spin-Orbit Coupling Effects in Strongly-Confined Electron Systems*, APS March Meeting 2010, Portland, OR, March 16, 2010
21. F. Bi, J. Levy, C. Cen, D. F. Bogorin, *Mechanism for writing and erasing nanostructures at the $LaAlO_3/SrTiO_3$ interface using vacuum AFM*, APS March Meeting 2010, Portland, OR, March 15, 2010
22. J.-W. Park, D. F. Bogorin, C. Cen, C. Nelson, Y. Zhang, C. W. Bark, C. Folkman, D. Felker, M. Rzchowski, X. Pan, J. Levy, C.-B. Eom, *Two-dimensional electron gas at $LaAlO_3/SrTiO_3$ heterointerfaces grown on silicon*, APS March Meeting 2010, Portland, OR, March 15, 2010
23. Y. Ma, P. Irvin, D. Bogorin, C. Cen, J. Levy, *Rewritable nanoscale photodetector at the $LaAlO_3/SrTiO_3$ interface*, APS March Meeting 2010, Portland, OR, March 15, 2010
24. S. Hu, J. Levy, C. Cen, D. F. Bogorin, *The effect of top $LaAlO_3$ surface treatment on the q-2DEGs at the $LaAlO_3/SrTiO_3$ interface*, APS March Meeting 2010, Portland, OR, March 15, 2010
25. D. F. Bogorin, C. Cen, J. Levy, *Rewritable superconducting nanostructures at the $LaAlO_3/SrTiO_3$ interface*, APS March Meeting 2010, Portland, OR, March 15, 2010
26. R. Garden, C. Cen, Jeremy Levy, *Low temperature Study of Oxide Nanostructures*, APS March Meeting 2010, Portland, OR, March 15, 2010
27. A. Burch, D. F. Bogorin, C. Cen, J. Levy, J.-W. Park, C.-B. Eom, *Nanoscale rectification at the $LaAlO_3/SrTiO_3$ interface*, APS March Meeting 2010, Portland, OR, March 15, 2010
28. P. Irvin, C. Cen, J. Levy, J.-W. Park, C.-B. Eom, *Energy dissipation of nanotransistors formed at the $LaAlO_3/SrTiO_3$ interface*, APS March Meeting 2010, Portland, OR, March 15, 2010
29. J. Levy, *Oxide Nanoelectronics on Demand*, MRS Spring Meeting 2010, San Francisco, CA, April 5, 2010
30. J. Levy, *Oxide Nanoelectronics on Demand*, California Institute for Technology, Pasadena, CA, April 13, 2010
31. J. Levy, *Oxide Nanoelectronics on Demand*, ICAM-I2CAM Meeting, Bangalore, India, April 20, 2010
32. J. Levy, *Oxide Nanoelectronics*, Carnegie Mellon University, Pittsburgh, PA, March 23, 2010
33. J. Levy, *Oxide Nanoelectronics*, Pennsylvana State University, University Park, PA April 29, 2010

ii. Non-Peer-Reviewed Conference Proceeding publications (other than abstracts)

(none)

iii. Peer-Reviewed Conference Proceeding publications (other than abstracts)

(none)

4. Manuscripts

1. P. Irvin, Y. Ma, D. F. Bogorin, C. Cen, C. W. Bark, C. M. Folkman, C.-B. Eom, J. Levy, *Rewritable nanoscale oxide photodetector*, submitted to Nature Photonics
2. C. Cen, D. F. Bogorin, J. Levy, *Thermal Activation and Quantum Tunneling in a Sketch-Based Oxide Nano Transistor*, submitted to Nano Letters
3. F. Bi, D. F. Bogorin, C. Cen, C.-B. Eom, J. Levy, *Mechanism for writing and erasing nanostructures at the $LaAlO_3/SrTiO_3$ interface*
4. J.-W. Park, D. F. Bogorin, C. Cen, C. T. Nelson, Y. Zhang, C. W. Bark, C. M. Folkman, D. Felker, M. Rzchowski, X. Pan, J. Levy, C.-B. Eom, *Two-dimensional electron gas at $LaAlO_3/SrTiO_3$ heterointerfaces grown on silicon*

5. Books

1. D. F. Bogorin, P. Irvin, C. Cen, J. Levy, "$LaAlO_3/SrTiO_3$-Based Device Concepts ", in *Oxide Nanoelectronics*, ed. Tsymbal, Eom, Ramesh, and Dagotto, Oxford University Press, Oxford, England, UK (in press)

6. Honor and Awards

1. Jeremy Levy: American Physical Society Fellow
2. Jeremy Levy: Aspen Center for Physics Public Lecture, *Etch-a-Sketch Nanoelectronics*: http://www.youtube.com/watch?v=OJnIh0iDf28

7. Title of Patents Disclosed during the reporting period

1. ON-DEMAND NANOELECTRONICS PLATFORM
   Application No: 61/262,693 filed November 19, 2009

8. Patents Awarded during the reporting period

(none)

(2) Student/Supported Personnel Metrics for this Reporting Period (name, % supported, %Full Time Equivalent (FTE) support provided by this agreement, and total for each category):

(a) Graduate Students

1. Feng Bi, 12 months at 100%

(b) Post Doctorates

1. Daniela Bogorin, 2 month at 100%
2. Shan Hu, 1 month at 100%

(c) Faculty

1. Jeremy Levy, 100%, 1 month

(d) Undergraduate Students

(none)

(e) Graduating Undergraduate Metrics (funded by this agreement and graduating during this reporting period):

N/A

i. Number who graduated during this period

ii. Number who graduated during this period with a degree in science, mathematics, engineering, or technology fields

iii. Number who graduated during this period and will continue to pursue a graduate or Ph.D. degree in science, mathematics, engineering, or technology fields

iv. Number who achieved a 3.5 GPA to 4.0 (4.0 max scale)

v. Number funded by a DoD funded Center of Excellence grant for Education, Research and Engineering

vi. Number who intend to work for the Department of Defense

vii. Number who will receive scholarships or fellowships for further studies in science, mathematics, engineering or technology fields

(f) Masters Degrees Awarded (Name of each, Total #)

(none)

(g) Ph.D.s Awarded (Name of each, Total #)

(none)

(h) Other Research staff (Name of each, FTE % Supported for each, Total % Supported)

(none)

(3) "Technology transfer" (any specific interactions or developments which would constitute technology transfer of the research results). Examples include patents, initiation of a start-up company based on research results, interactions with industry/Army R&D Laboratories or transfer of information which might impact the development of products.

(none)

(4) Scientific Progress and Accomplishments (description should include significant theoretical or experimental advances)

Overview

We report progress in creating nanoscale transistors at the $LaAlO_3/SrTiO_3$ interface using a rewritable conductive AFM technique. We have created $LaAlO_3/SrTiO_3$-based nano-transistors (SketchFETs) that operate at GHz frequencies. We have also demonstrated nanoscale phototransistors that are spectrally sensitive to visible and near-infrared light. We have also investigated the creation of "designer potential barriers" that allow the creation of nanoscale diodes. Finally, we have tested a physical model of the AFM writing mechanism, which shows that water vapor is an essential component to make these structures - an important step in developing devices in this material. For the remaining period we will further investigate the high frequency properties and SketchFETs, with a goal of quantifying power dissipation per drive cycle in these devices. We will also continue to develop single-electron transistor devices.

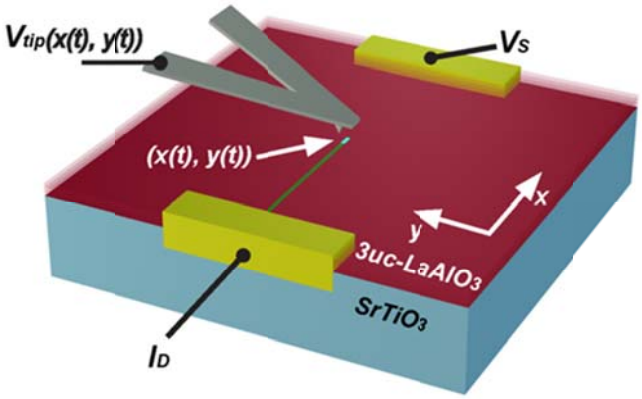

Figure 1 Illustration of nanowire writing at the $LaAlO_3/SrTiO_3$ interface. Buried Au electrodes (shown in yellow) are directly contacted to the $LaAlO_3/SrTiO_3$ interface. The AFM tip with an applied voltage is scanned once between the two electrodes with a voltage applied $V_{tip}(x(t),y(t))$. Positive voltages locally switch the interface to a conducting state, while negative voltages locally restore the insulating state. Here, a conducting nanowire (shown in green) is being written. The conductance between the two electrodes is monitored by applying a small voltage bias on one of the two gold electrodes (V_S) and reading the current at the second electrode (I_D).

Background

Epitaxial growth of $LaAlO_3$ on $SrTiO_3$ can lead to an unusual and energetically unstable charge distribution. One predicted consequence of the polar discontinuity between $LaAlO_3$ and $SrTiO_3$ is an interfacial insulator-to-metal transition that is dependent on the $LaAlO_3$ thickness. This effect occurs in structures of $LaAlO_3$ grown on TiO_2-terminated $SrTiO_3$. When $LaAlO_3$ is grown with greater than a critical thickness d_c = 3 unit cell (uc), the interface between $LaAlO_3$ and $SrTiO_3$ is found to be conducting. When the thickness of $LaAlO_3$ is smaller than d_c the interface remains insulating. In samples grown with approximately 3 uc of $LaAlO_3$ (normally insulating), the interface can be switched between the insulating and conducting states by applying a voltage to the back of the $SrTiO_3$ substrate or to the top of the $LaAlO_3$.

A powerful method for creating nanoscale devices at the $LaAlO_3/SrTiO_3$ interface involves metastable charging of the top $LaAlO_3$ surface with a conducting AFM probe (Figure 1). By locally and reversibly controlling a metal-insulator transition, the creation of both isolated and continuous conducting features has been demonstrated with length scales smaller than 2 nm. These structures can be erased and rewritten numerous times. As a result of the enormous flexibility in controlling electronic properties at near-atomic dimensions, a variety of nanoscale devices can be realized.

GHz switching of SketchFETs

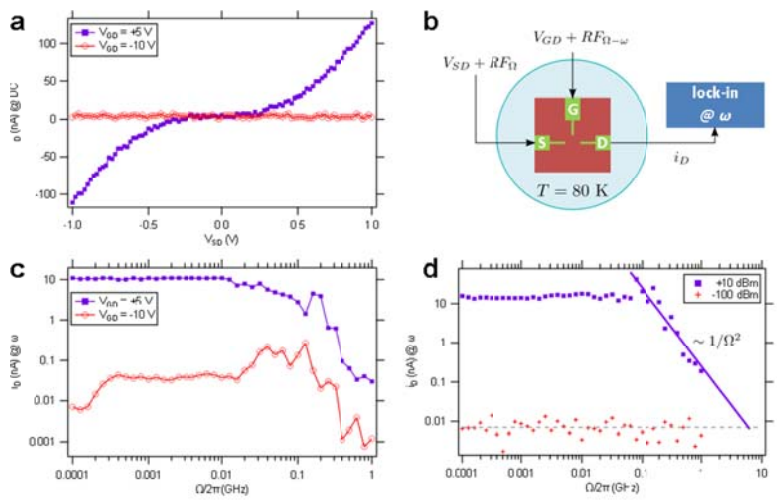

Figure 2 GHz SketchFET.(a) *I-V* curve of device at V_{GD} = +5 V and -10 V. (b) Diagram of heterodyne detection experiment. (c) Drain current measured at the difference frequency ω as a function of RF frequency Ω. V_{SD} = +1 V and P_{RF} = 0 dBm. (d) Frequency response showing cutoff frequency ω_T at approximately 4.6 GHz.

One gauge of the performance of a transistor is its ability to modulate or amplify signals at high frequencies, as quantified by the cutoff frequency ω_T. Characterization of the frequency dependence of the SketchFET is done using a heterodyne circuit that incorporates the SketchFET as a frequency mixer. The experimental arrangement is shown schematically (b). In addition to a DC bias that can tune the background conductance, the source electrode (ie, RF port) and gate electrode (LO port) are driven with continuous-wave RF signals of power P_{RF} at frequencies Ω and Ω - ω, respectively. The current at the drain electrode (IF port) is measured on a lock-in amplifier at the difference frequency ω. Because this is a background-free measurement, only in the case where the SketchFET operates as a frequency mixer will there be a signal of frequency ω at the drain electrode.

In prior work to characterize the frequency response of a SketchFET, ω_T was found to be on the order of 15 MHz and the limiting factor was mainly attributed to the resistance in the leads (R_S = 1 MΩ). By widening the leads from 12 to 100 nm we have decreased the lead resistance to 500 kΩ. Performing the heterodyne measurement described above demonstrates operation of a SketchFET at GHz frequencies ((c)). By extrapolating a $1/\Omega^2$ dependence, we estimate a cutoff frequency of 4.6 GHz.

Nanoscale phototransistors

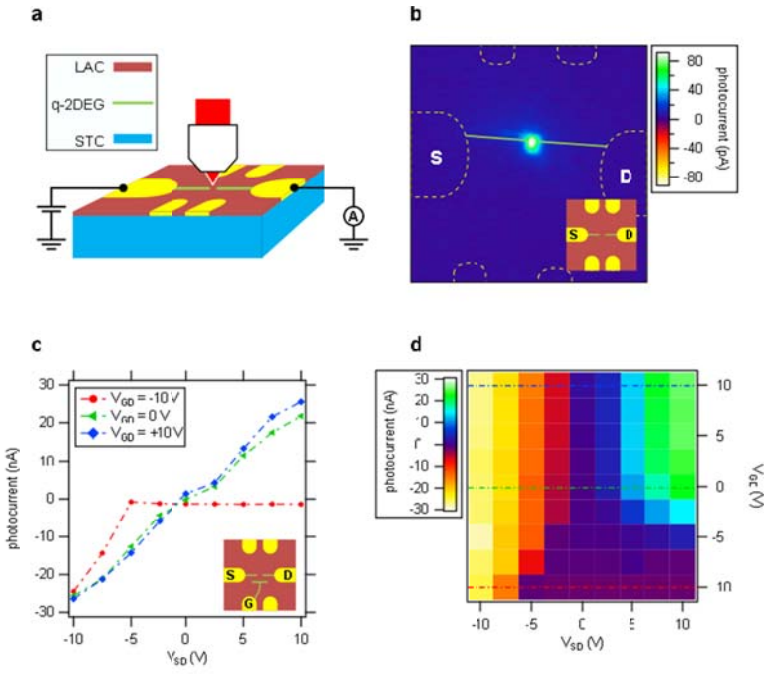

Figure 3 (a) Diagram of photocurrent measurement. (b) Scanning photocurrent microscopy (SPCM) image of two-terminal device shown in inset. $I \sim 30$ kW/cm^2 ($NA = 0.73$), $V_{SD} = 0.1$ V, $T = 300$ K. (c) Photocurrent vs. VSD of the three-terminal device shown in the inset. I ~ 20 W/cm2 ($NA = 0.13$), $T = 80$K. (d) Intensity map of photocurrent of three-terminal device as a function of V_{SD} and V_{GD}.

In addition to the transistors described above, one can also use AFM patterning of the $LaAlO_3/SrTiO_3$ interface to create rewritable, nanoscale phototransistors. Nanophotonic devices seek to generate, guide, and/or detect light using structures whose nanoscale dimensions are closely tied to their functionality. Although semiconducting nanowires, grown with tailored optoelectronic properties, have been successfully placed into devices for a variety of applications, the integration of photonic nanostructures with electronic circuitry remains one of the most challenging aspects of device development. The rewritable nanoscale phototransistors described here exhibit a remarkably high gain for their size and possess an electric field-tunable spectral response spanning the visible-to-near-infrared regime.

Optical properties of nanostructures are characterized by fixed position photocurrent measurements and spatially mapped using scanning photocurrent microscopy (SPCM) (Figure 3 (a)). The intensity of a laser source is modulated by an optical chopper at frequency f_R; the resulting photocurrent i_{PC} is collected from a drain electrode and measured with a lock-in amplifier at f_R. When the light overlaps with the device a sharp increase in the photocurrent is observed.

The simplest nanophotonic device consists of a nanowire with a narrow gap or junction, which can be deterministically placed with nanometer-scale accuracy. An SPCM image shows spatially-localized photocurrent detected only in the region of the junction (Figure 3 (b). The devices are erasable and reconfigurable and furthermore are not damaged by illuminating with

kW/cm^2 intensity: following optical characterization, devices may be erased and rewritten. The photosensitivity can be optically modulated at frequencies as high as 3.5 kHz and the response appears limited by the RC time constant of the device.

The functionality of these devices can be extended by adding an independent gate electrode using the same geometry as the previously discussed SketchFET. This bias V_{GD} can be used to modify the source-drain conductance, enabling conduction between source and drain for positive V_{GD} and inhibiting it for negative V_{GD} (Figure 3 (c)). Photocurrent measured as a function of V_{SD} and V_{GD} (Figure 3 (d)), exhibits a polarity that is always the same sign as the V_{SD}, irrespective of V_{GD}, indicating that there is negligible leakage current from the gate to the drain. Furthermore, the photocurrent is suppressed when both V_{SD} is positive and V_{GD} is negative, demonstrating the ability of the gate electrode to tune the photoconductivity in the source-drain channel.

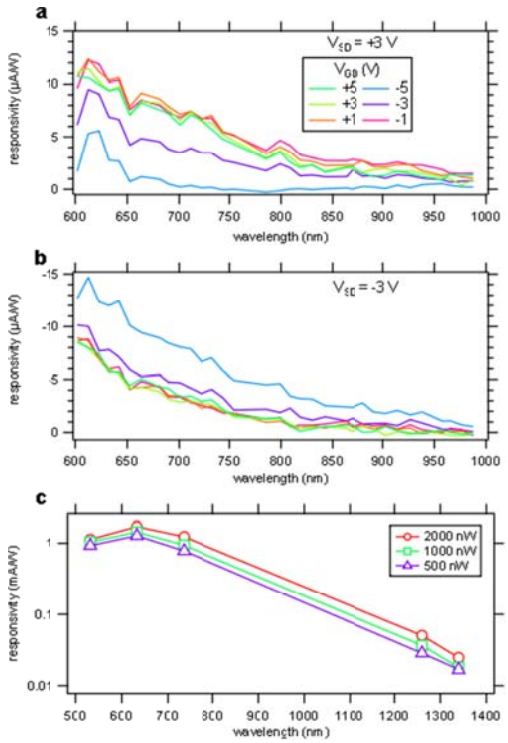

Figure 4 Gate-controlled spectral response of phototransistor. Fixed-position photocurrent as a function of λ and V_{GD} for (a) V_{SD} = +3 V and (b) V_{SD} = -3 V. (a) and (b): NA = 0.28, T = 300 K. (c) Responsivity of photodetector from 532 nm to 1340 nm. Lines are guides to the eye. V_{SD} = +2 V, V_{GD} = 0 V, NA = 0.13, T = 80 K.

To investigate the wavelength dependence of these devices, we use a variety of fixed-wavelength lasers (532 nm, 633 nm, 735 nm, 1260 nm, and 1340 nm) and also a supercontinum white light source (600 - 1000 nm) derived from Ti:Sapphire laser. The spectral response (Figure 4) is sensitive to V_{SD} and V_{GD}. At positive V_{SD} the phototransistor response red-shifts as the gate bias is increased. A similar Stark shift is observed when sweeping the source bias. This evidence of a Stark effect, along with finite element analysis showing that the electric field is predominantly confined to the gap region, indicates that the photo-induced absorption is highly localized. Remarkably, the photosensitivity extends to 1340 nm, the longest wavelength investigated. Analysis of noise equivalent target (NET) shows a minimum NET of 11 mW/cm^2/√Hz (T = 80 K and λ = 735 nm).

The rewritable phototransistors presented here bring new functionality to oxide nanoelectronics. For example, existing nanowire-based molecular sensors rely on the ability to bring the analyze into contact with the sensing area of the detector. Here the roles are reversed: a nanoscale phototransistor can be placed in intimate contact with an existing molecule or biological agent. It may be possible to take advantage of the significant Stark-shifted photoresponse to improve the spatial sensitivity well beyond the diffraction limit. The ability to integrate optical and electrical components such as nanowires and transistors may lead to devices that combine in a single platform sub-wavelength optical detection with higher-level electronics-based information processing.

Designer Potential Barriers

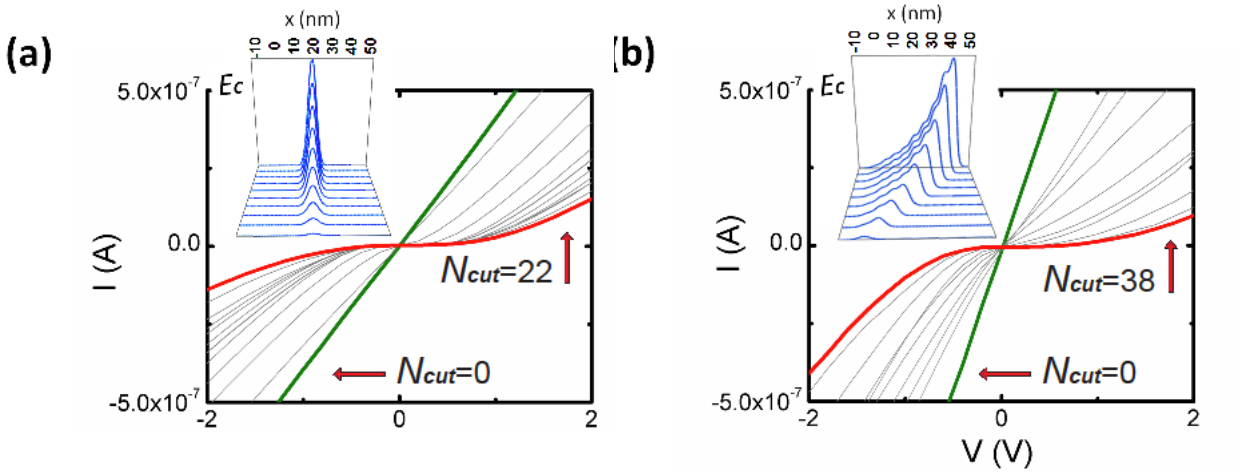

Figure 5 Creation of designer potential barriers. (a) I-V plots for a nanowire cut at the same location multiple times with an AFM tip bias V_{tip} = -2 mV. The green curve indicates the *I-V* curve before the first cut. Intermediate *I-V* curves are shown after every alternate cut. As the wire is cut, the potential barrier increases (inset) and the zero-bias conductance decreases; however, the overall *I-V* curve remains highly reciprocal. (b) *I-V* plots for a nanowire subject to a sequence of cuts $N_{cut}(x)$ at nine locations spaced 5 nm apart along the nanowire. The green curve indicates *I-V* curve before the first cut. The asymmetry in $N_{cut}(x)$ results in a non-reciprocal *I-V* curve.

The high degree of control over the energy landscape within the $LaAlO_3/SrTiO_3$ 2DEG allows for the development of a variety of nonlinear devices such as nanoscale junctions. The shape of the barrier can determine whether the transport is reciprocal ($I(V) = -I(-V)$) or rectifying.

The controlled creation of rectifying structures is further described below. Non-reciprocal nanostructures can be created using a slightly different c-AFM manipulation. In this approach, spatial variations in the conduction-band profile are created by a precise sequence of erasure steps. In a first experiment, a conducting nanowire is created using V_{tip} = +10 V. The initial *I-V* curve (Figure 5 (a), green curve) is highly linear and reciprocal. This nanowire is then cut by scanning the AFM tip across the nanowire at a speed v_y = 100 nm/s using V_{tip} = -2 mV at a fixed location (x = 20 nm) along the length of the nanowire. This erasure process increases the conduction-band minimum $E_c(x)$ locally by an amount that scales monotonically with the number of passes N_{cut} (Figure 5 (a), inset); the resulting nanostructure exhibits a crossover from conducting to activated to tunneling behavior. Here we focus on the symmetry of the full *I-V* curve. As N_{cut} increases, the transport becomes increasingly nonlinear; however, the *I-V* curve remains highly reciprocal. The canvas is subsequently erased and a uniform conducting nanowire is written in a similar fashion as before (V_{tip} = +10 V, v_x = 400 nm/s). A similar erasure sequence is performed; however, instead of cutting the nanowire at a single x coordinate, a sequence of cuts is performed at nine adjacent x coordinates along the nanowire (separated by D_x = 5 nm). The number of cuts at each location along the nanowire $N_{cut}(x)$ increases monotonically with x, resulting in a conduction band profile E_c(x) that is asymmetric by design (Figure 5 (b), inset). The resulting *I-V* curve for the nanostructure evolves from being highly linear and reciprocal before writing (Figure 5 (b), (green curve)) to highly nonlinear and non-reciprocal (Figure 5 (b), red curve).

Nanoscale control over asymmetric potential profiles at the interface between $LaAlO_3$ and $SrTiO_3$ can have many potential applications in nanoelectronics and spintronics. Working as straightforward diodes, these junctions can be used to create half-wave and full-wave rectifiers for AC-DC conversion or for RF detection and conversion to DC. By cascading two or more such junctions, with a third gate for tuning the density in the intermediate regime could form the basis for low-leakage transistor devices. The ability of controlling the potential along a nanowire could also be used to create wires with built-in polarizations similar to those created in heterostructures that lack inversion symmetry.

Mechanism for writing and erasing nanostructures at the $LaAlO_3/SrTiO_3$ interface

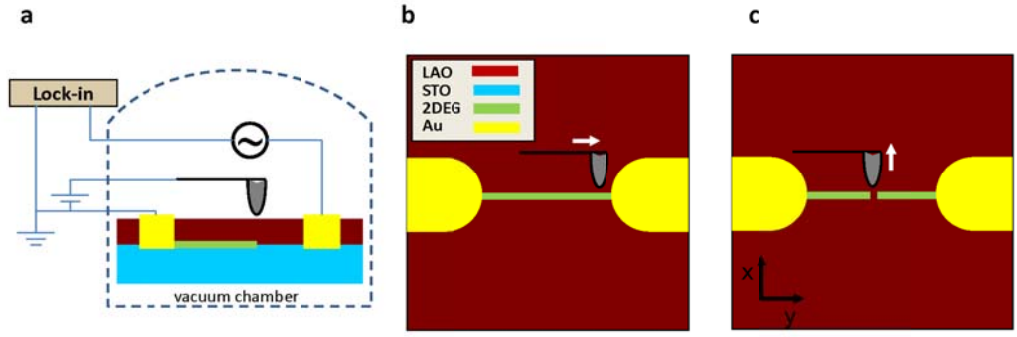

Figure 6 Writing and erasing nanowires at 3 uc $LaAlO_3/SrTiO_3$ interface. (a) Side view schematic illustrating a conducting AFM probe writing a nanowire in a controlled environment. (b) Top view schematic of a writing experiment in which a nanowire is created with a positive biased tip. (c) Top view schematic of a cutting experiment in which a nanowire is locally erased with a negatively biased tip.

A physical understanding of the writing and erasing mechanism is not only important for fundamental reasons but also for the development of future technologies that are based on the stability of these nanostructures. Conducting islands with densities >150 Tb/in^2 have been demonstrated and transistors with channel lengths of 2 nm have been reported. An understanding of the physical original of these astonishing results can help in the development of conditions that can stabilize these structures over time scales that are relevant for information storage and processing applications (i.e., ~10 years).

One proposed mechanism for the writing process involves the adsorption of H_2O dissociating into OH^- and H^+ on the $LaAlO_3$ surface. A conducting AFM tip provides a means to locally modify the population of charged OH^- and H^+ adsorbates. This form of modulation doping locally switches the $LaAlO_3/SrTiO_3$ interface between the insulating and conducting states. During the writing process a positively-charged AFM probe removes OH^- adsorbates, thus locally charging the top surface with the H^+ ions that remain which therefore creates a conducting interface. During the erasing process, a negatively-charged AFM probe removes H^+ adsorbates, restoring the interface to an insulating state. We refer to this process as a "water cycle" because it permits multiple writing and erasing without physical modification of the oxide heterostructure.

We have investigated the writing and erasing process under a variety of atmospheric conditions in order to constrain the physical models of the writing and erasing procedure. To perform these experiments, we use a vacuum AFM (Figure 6 (a)). It is capable of operation down to 10^{-5} Torr and allows for the controlled introduction of various gases. Writing and erasing experiments (Figure 6 (b,c)) are performed in different atmospheres while the stability of nanostructures is monitored in real time as the ambient gaseous environment is modified. Prior to the writing, the $LaAlO_3$ surface is alternatively raster-scanned with $V_{tip} = \pm 10$ V to remove any adsorbates on the $LaAlO_3$ surface and thus "initialize" the surface.

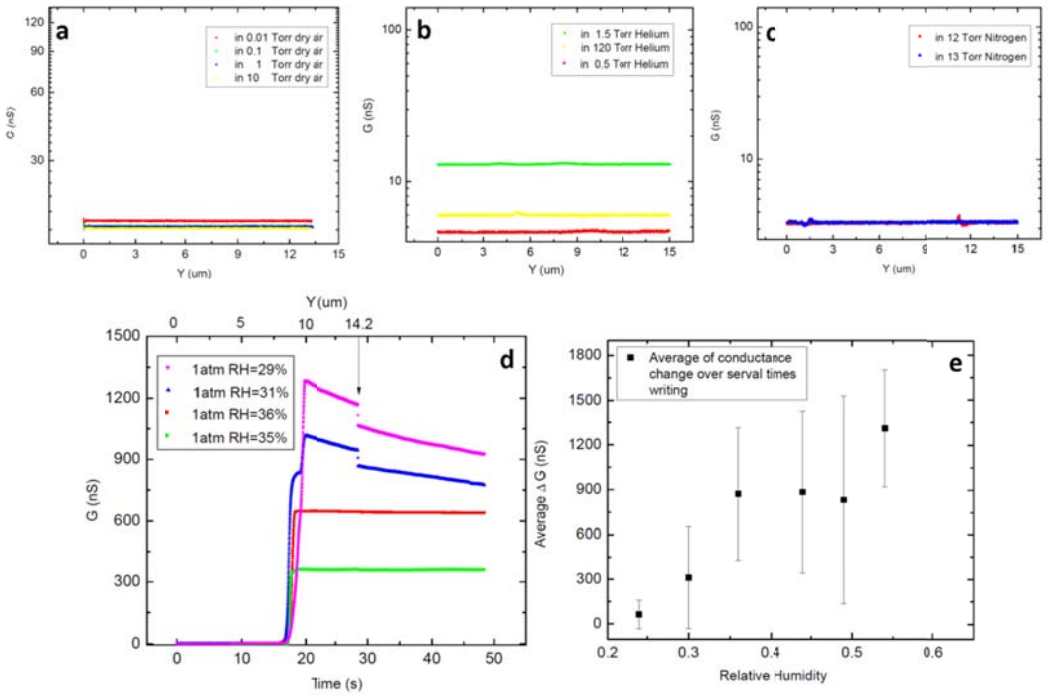

Figure 7 Nanowire writing under various atmospheric conditions. Writing a nanowire in (a) air, (b) helium, or (c) nitrogen environments does not result in a conducting nanowire. (d) Writing in different relative humidity (RH) level of air at 1atm. (e) Influence of RH on writing ability. All experiment are performed at $T = 295$ K.

A straightforward test of the "water cycle" mechanism outlined above replaces atmospheric conditions with gas environments that lack H_2O. Figure 7 (a-c) shows the results of a number of writing experiments performed using dry air (Figure 7 (a)), helium (Figure 7 (b)), and nitrogen (Figure 7 (c)) with pressures ranging from 10^{-2} - 10^{2} Torr. Nanowires were not formed under any of these conditions. Similarly, nanowires were not formed under vacuum conditions. Next, writing experiments are performed under various conditions of relative humidity (RH). The results shown in Figure 7 (d) establish that water must be present for conducting nanostructure writing.

(5) "Copies of technical reports," which have not been previously submitted to the ARO, should be submitted concurrently with the Interim Progress Report. (See page 6 "Technical Reports" section for instructions.) However, do not delay submission while awaiting Reprints of publications.